# Photoactivation mechanism of PAmCherry based on crystal structures of the protein in the dark and fluorescent states

Fedor V. Subach[a,1], Vladimir N. Malashkevich[b,1], Wendy D. Zencheck[b], Hui Xiao[c], Grigory S. Filonov[a], Steven C. Almo[b], and Vladislav V. Verkhusha[a,2]

[a]Department of Anatomy and Structural Biology and Gruss-Lipper Biophotonics Center, and Departments of [b]Biochemistry and [c]Pathology, Albert Einstein College of Medicine, Bronx, NY 10461

Edited by Jennifer Lippincott-Schwartz, National Institutes of Health, Bethesda, MD, and approved October 14, 2009 (received for review August 13, 2009)

**Photoactivatable fluorescent proteins (PAFPs) are required for super-resolution imaging of live cells. Recently, the first red PAFP, PAmCherry1, was reported, which complements the photoactivatable GFP by providing a red super-resolution color. PAmCherry1 is originally "dark" but exhibits red fluorescence after UV-violet light irradiation. To define the structural basis of PAmCherry1 photoactivation, we determined its crystal structure in the dark and red fluorescent states at 1.50 Å and 1.65 Å, respectively. The non-coplanar structure of the chromophore in the dark PAmChery1 suggests the presence of an N-acylimine functionality and a single non-oxidized $C^{\alpha}$-$C^{\beta}$ bond in the Tyr-67 side chain in the cyclized Met-66-Tyr-67-Gly-68 tripeptide. MS data of the chromophore-bearing peptide indicates the loss of 20 Da upon maturation, whereas tandem MS reveals the $C^{\alpha}$–N bond in Met-66 is oxidized. These data indicate that PAmCherry1 in the dark state possesses the chromophore *N*-[(E)-(5-hydroxy-1*H*-imidazol-2-yl)methylidene]acetamide, which, to our knowledge, has not been previously observed in PAFPs. The photoactivated PAmCherry1 exhibits a non-coplanar anionic DsRed-like chromophore but in the *trans* configuration. Based on the crystallographic analysis, MS data, and biochemical analysis of the PAmCherry1 mutants, we propose the detailed photoactivation mechanism. In this mechanism, the excited-state PAmCherry1 chromophore acts as the oxidant to release $CO_2$ molecule from Glu-215 via a Koble-like radical reaction. The Glu-215 decarboxylation directs the carbanion formation resulting in the oxidation of the Tyr-67 $C^{\alpha}$-$C^{\beta}$ bond. The double bond extends the $\pi$-conjugation between the phenolic ring of Tyr-67, the imidazolone, and the N-acylimine, resulting in the red fluorescent chromophore.**

chromophore | localization microscopy | photoconversion

Super-resolution imaging approaches such as photoactivation localization microscopy provide the ability to observe details of cellular and even macromolecular structure that were not previously discernible with less than 40 nm resolution (1). There is significant demand for a broader and more diverse range of photoactivatable fluorescent probes (2), in particular irreversibly photoactivatable fluorescent proteins (PAFPs). To develop PAFPs with new spectral properties, it is essential to gain understanding of the underlying mechanisms of photoactivation.

X-ray structures have been reported for a number of irreversible PAFPs, including those that change their fluorescence from green to red upon irradiation with violet light such as EosFP (3), its derivative IrisFP (4), Kaede (5), KikGR (6), and Dendra2 (7). These PAFPs share the same His-Tyr-Gly chromophore-forming tripeptide and the same mechanism of photoactivation. This mechanism is associated with a $\beta$-elimination reaction, which results in the cleavage of the peptide bond between the amide nitrogen and $\alpha$-carbon of the His residue in the chromophore tripeptide (8).

Another group of irreversible PAFPs includes photoactivatable GFP (PAGFP) (9), photoswitchable CFP (10), and its derivative photoswitchable CFP2 (11). This group of PAFPs is capable of irreversible photoconversion from the neutral (i.e., protonated) to anionic (i.e., deprotonated) states of the chromophore. Photoactivation mechanism of these PAFPs consists of a decarboxylation of the Glu-215 residue (for numbering of the amino acid residues, see Fig. S1), resulting in reorganization of the hydrogen bond network inside the protein $\beta$-barrel and chromophore deprotonation. The crystal structure of PAGFP supports this mechanism (12).

PAmCherry1 PAFP (13) is a derivative of the mCherry RFP, which contains 10 aa substitutions (Fig. S1). It irreversibly photoconverts from a dark state (i.e., OFF state) to the red fluorescent state (i.e., ON state) in response to the violet light irradiation. The lack of fluorescence in the OFF state and single-molecule behavior makes monomeric PAmCherry1 a preferred red probe for photoactivation localization microscopy.

Here, we report crystal structures of PAmCherry1 in the OFF and ON states, MS data, and spectral and biochemical characterization of the PAmCherry1 mutants. The data have revealed the chemical structure of the PAmCherry1 chromophore in both states and suggest a mechanism for PAmCherry1 photoactivation.

## Results

**Overall Structure of the PAmCherry1 Protein.** The crystal structures of PAmCherry1 in the OFF and ON states were refined at 1.5 Å and 1.65 Å resolution, respectively (Table S1). In both isomorphous structures, the asymmetric unit contains one PAmCherry1 protein chain with total solvent accessible area of approximately 9,880 $Å^2$ (Fig. S2). Contacts between symmetry-related protein chains are not extensive, so, in contrast to some other fluorescent proteins, PAmCherry1 remains monomeric in the crystal form. Most of the residues of polypeptide chain (Ala-6 through Ser-222) are well defined in the electron density map. In both structures, all residues are within the favorable area of the Ramachandran plot. PAmCherry1 molecules in the ON and OFF states have overall temperature factors of 21.6 and 27.8 $Å^2$, respectively. PAmCherry1 and the parental mCherry structures are similar, with rmsds between the all $C^{\alpha}$ atoms of 1.3 Å for both OFF and ON states. Protein chain is folded into the characteristic 11-stranded $\beta$-barrel, described previously for GFP, DsRed (14), and mCherry (15), in which the central $\alpha$-helix containing the chromophore is extended coaxially with the axis of the $\beta$-barrel (Fig. S2). Notably, 2 $\beta$-strands

Author contributions: V.V.V. designed research; F.V.S., V.N.M., W.D.Z., and H.X. performed research; F.V.S., V.N.M., W.D.Z., H.X., and G.S.F. analyzed data; and F.V.S., S.C.A., and V.V.V. wrote the paper.

The authors declare no conflict of interest.

This article is a PNAS Direct Submission.

Data deposition: The atomic coordinates and structural factors have been deposited in the Protein Data Bank, www.pdb.org (PDB ID codes are 3KCS for PAmCherry1 in the dark state and 3KCT for PAmCherry1 in the fluorescent state).

[1]F.V.S. and V.N.M. contributed equally to this work

[2]To whom correspondence should be addressed. E-mail: vladislav.verkhusha@einstein.yu.edu.

This article contains supporting information online at www.pnas.org/cgi/content/full/0909204106/DCSupplemental.

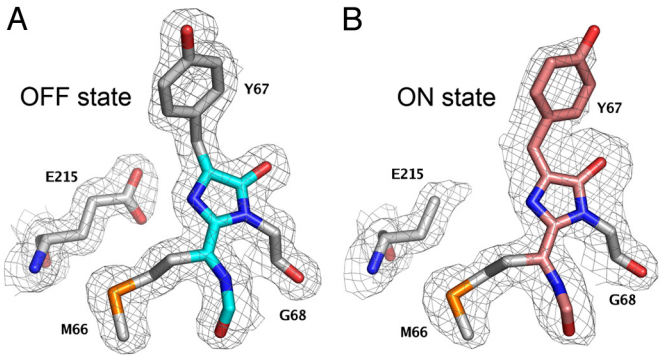


**Fig. 1.** Structures of the PAmCherry1 chromophore in the OFF (*A*) and ON (*B*) states superimposed onto the respective experimental $2F_o$-$F_c$ electron density maps (contoured at 1$\sigma$) are shown. The chromophore moiety is shown in stick representation colored in cyan (OFF state) or pink (ON state), respectively. More diffused electron density indicates that traces of the OFF state and some intermediate conformations may be present in the ON state.

within the barrel have irregular structure near residues Ala-145 and Pro-163, i.e., in the area facing the hydroxyphenyl ring.

**Chromophore and Environment of PAmCherry1 in the Dark State.** Electron density of the PAmCherry1 Met-66-Tyr-67-Gly-68 tripeptide in the OFF state is consistent with the formation of an imidazolone heterocycle (Fig. 1*A* and Fig. 2*A*). An observed planar geometry of $C^{\alpha}$ atom of Tyr-67 suggests its $sp^2$ hybridization. Both the formation of hydrogen bond between the hydroxyl group of imidazol-5-ol and the guanidinium group of Arg-95 and the conjugation of enol with the adjacent N=C double bond possibly stabilize the enol tautomer in the keto-enol equilibrium. Imidazole-5-ol is derivative of imidazole, which has a p$K_a$ of approximately 7; consequently, imidazole-5-ol can be protonated by Glu-215 with a p$K_a$ of approximately 4. Glu-215 is close to the $N^3$ atom of the imidazole-5-ol and, in its minor alternative conformation (see Fig. 2 legend), forms hydrogen bond with it. The similar contact has been observed in other RFPs including mCherry (15) and eqFP611 (16).

Analysis of the crystal structure in the OFF state revealed that the hydroxyphenyl group in the PAmCherry1 chromophore is in a non-coplanar conformation with a $\chi_1$ of 90° ± 4° and $\chi_2$ of −82° ± 4° (Fig. 1*A*). As none of the torsion angles is 0° or 180°, the $C^{\beta}$ atom in Tyr-67 has $sp^3$ hybridization, not $sp^2$ hybridization as observed in mCherry (15). This suggests that PAmCherry1 in the OFF state has a single bond, not a double bond, between the $C^{\beta}$ atom in Tyr-67 and the imidazol-5-ol ring. The absence of the Tyr-67 $C^{\alpha}$-$C^{\beta}$ double bond results in a lack of conjugation between the 2 aromatic rings and, subsequently, in a shift of the absorbance from 590 nm in parental mCherry to 405 nm in PAmCherry1.

Electron density around the $C^{\alpha}$ atom of Met-66 is planar, suggesting its $sp^2$ hybridization. Consequently, the PAmCherry1 chromophore in the OFF state possibly has an N-acylimine group with the double bond between the $C^{\alpha}$ and N atoms of Met-66. This was further confirmed by a MS analysis (described later). Similarly to mCherry (15) and DsRed (17), the Phe-65-Met-66 peptide bond in PAmCherry1 is close to *cis* conformation ($\omega = -78° \pm 10°$). This transition state conformation indicates that the peptide bond is transformed into a single bond; and the released electrons are used to form the double N-$C^{\alpha}$ bond in Met-66. The value of Met-66 $\varphi$ of 155° ± 10° is consistent with double nature of the N-$C^{\alpha}$ bond (an ideal $\varphi$ is 180°). The change in the $\omega$ angle after the photoactivation (described later) can possibly slightly increase the chromophore brightness and shift its emission to longer wavelengths because of the improved conjugation of the chromophore with the carbonyl group of N-acylimine. It has been suggested for DsRed that formation of the N-acylimine is coupled to the peptide bond isomerization (18). Thus, electron density of PAmCherry1 in the OFF state is consistent with the post-translational modification of the Met-66-Tyr-67-Gly-68 tripeptide resulting in the formation of the 4-(4-hydroxybenzyl)-imidazol-5-ol and N-acylimine groups.

The PAmCherry1 chromophore in the OFF state is involved in multiple interactions within the $\beta$-barrel interior (Fig. 2*A*). It forms 22 contacts with a 4-Å distance cutoff (Gln-42, Thr-43, Ala-44, Ser-62, Pro-63, Gln-64, Phe-65, Ser-69, Asn-70, Trp-93, Arg-95, Gln-109, Trp-143, Pro-163, Arg-197, Leu-199, Gln-213, and 5 water molecules), of which 5 are hydrogen bonds (Pro-63 O-N Gly-68, Gly-68 O–Wat, Gly-68 O–Wat, Tyr-67 O–$N_{\eta 2}$ Arg-95, Tyr-67 O–Wat) and the rest are van der Waals contacts.

The aliphatic side chain of Met-66 in the chromophore tripeptide Met-Tyr-Gly forms van der Waals contacts with the side chains of Gln-42, Ala-44, Leu-199, Gln-213, and Glu-215 and the main chain of Thr-43. The hydroxyl group of the imidazol-5-ol chromophore moiety forms hydrogen bonds with the Arg-95 side chains and

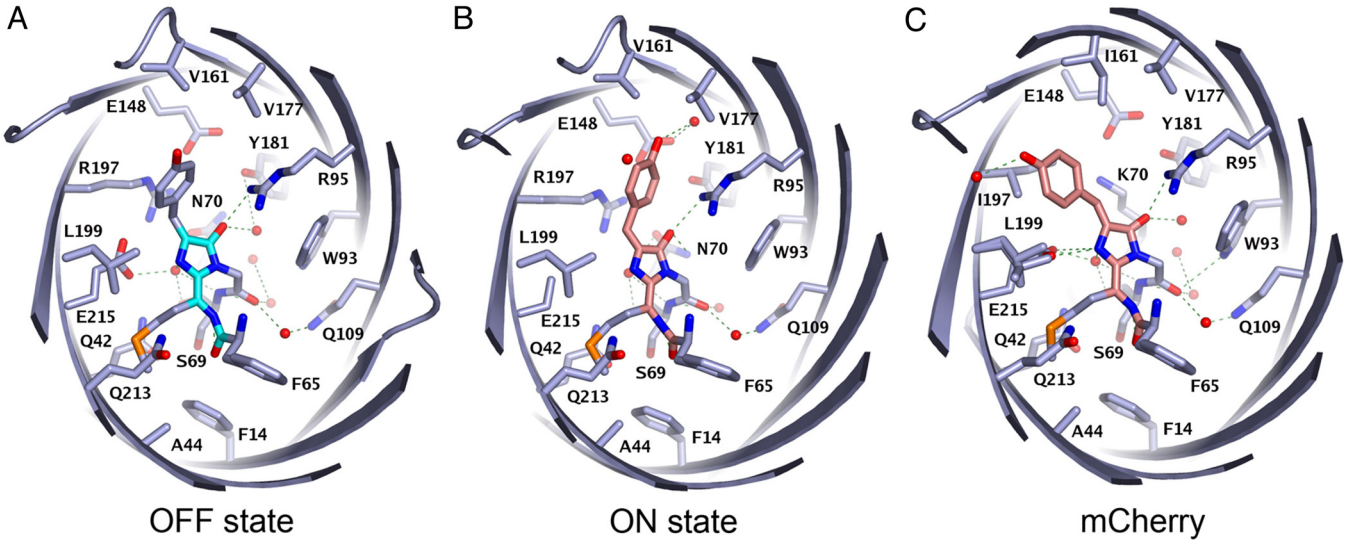


**Fig. 2.** Structures of the PAmCherry1 chromophore within its environment in the OFF (*A*) and ON (*B*) states. Water molecules are shown as red spheres; hydrogen bonds are shown as green dashed lines. The mCherry chromophore and its environment (PDB ID code 2H5Q) are shown for comparison (*C*).

water. The glycyl moiety in the chromophore makes van der Waals contacts with Trp-93 and hydrogen bonds with 2 waters.

The *p*-hydroxyphenyl group in the non-coplanar conformation of the chromophore is not involved in any hydrogen bonds; and its hydroxyl group might be protonated under the crystallization conditions (pH 8.5). The position of the *p*-hydroxyphenyl group is stabilized via van der Waals contacts with Pro-63, Leu-199, Trp-143, and Pro-163. Three of 5 water molecules are in proximity to the chromophore and form hydrogen bonds with it. Positions of these water molecules are additionally stabilized through hydrogen bonds with the Ser-111 hydroxyl group, the Gln-109 amino group, main chain of Gln-64 and Gly-68, and other water molecules. Two of 5 water molecules, which did not form contacts with the chromophore, form hydrogen bonds with the Asn-70 main and side chains and other water molecules.

**Chromophore and Environment of PAmCherry1 in the Fluorescent State.** To determine crystal structure of PAmCherry1 in the photoactivated state, we illuminated the crystals with 405 nm light until the maximal increase of the red fluorescence. Electron density of the PAmCherry1 Met-66-Tyr-67-Gly-68 tripeptide in the ON state is consistent with the formation of the imidazolone heterocycle. A planar geometry of the $C^{\alpha}$ atom of Met-66 suggests presence of the N-acylimine group (Fig. 1*B*). Similarly to that observed in mCherry (15), the Phe-65-Met-66 peptide bond in PAmCherry1 is close to the *cis* conformation ($\omega$ of $-28° \pm 10°$) that correlates with the formation of the N-acylimine. The $C^{\beta}$ atom of Tyr-67 has geometry more close to planar, suggesting formation of the $C^{\alpha}$-$C^{\beta}$ double bond in Tyr-67. Therefore, a PAmCherry1 red chromophore is possibly formed as the result of the conjugation of the 5-midazol-4-one group with the N-acylimine and hydroxyphenyl groups. In other words, the photoactivated PAmCherry1 has the DsRed-like chromophore but with the *trans* configuration of the double bond between the $C^{\alpha}$ atom of Tyr-67 and imidazolone ring with an $\chi_1$ of $156° \pm 4°$ and $\chi_2$ of $51° \pm 4°$ (Fig. 1*B*). The detected slight non-coplanarity may results from a mixture of the PAmCherry1 molecules in the crystal photoactivated to different extents. However, the photoactivated PAmCherry1 indeed has a slightly non-coplanar chromophore as it has been shown for several other RFPs such as Rtms5 (16) and KFP (19).

The substantially reduced electron density of the Glu-215 carboxyl group of the photoactivated PAmCherry1 suggests a light-induced decarboxylation of Glu-215 (Fig. 1*B*). The decarboxylation of Glu-215 has been observed in PAGFP (12).

The PAmCherry1 chromophore in the ON state forms 25 contacts less than 4 Å with the $\beta$-barrel interior (Fig. 2*B*), including 17 contacts, which were observed in the dark protein (Gln-42, Ala-44, Ser-62, Pro-63, Gln-64, Phe-65, Ser-69, Asn-70, Trp-93, Arg-95, Gln-109, Arg-197, Gln-213, and 4 water molecules). The chromophore forms 7 new contacts (Phe-14, Glu-148, Val-161, Val-177, Tyr-181, and 2 water molecules). The chromophore in the ON state forms 5 hydrogen bonds (Pro-63 O-N Gly-68, Gly-68 O–Wat, Gly-68 O–Wat, Tyr-67 $O_{\eta}$–Wat, Tyr 67 O–$N_{\eta 2}$ Arg-95, and Tyr-67 O–$N_{\delta 2}$ Asn-70) and the rest are van der Waals contacts.

The hydrophobic side chain of Met-66 within the chromophore tripeptide Met-Tyr-Gly rests in a pocket formed by the side chains of Phe-14, Gln-42, Ala-44, Ser-62, Phe-65, Leu-199, Gln-213, and Glu-215. This pocket is conserved among RFPs (14, 16, 19, 20).

The carbonyl group of the imidazolone ring in the chromophore forms hydrogen bonds with the side chains of Asn-70 and Arg-95 and 2 water molecules. In the ON state, the Asn-70 residue has replaced a water molecule, which formed the hydrogen bond with the carbonyl group in the OFF state. In addition, the glycyl moiety in the chromophore makes van der Waals contacts with Pro-63, Gln-64, Phe-65, Ser-69, Asn-70, Trp-93, and Gln-109.

The *p*-hydroxyphenyl group makes van der Waals contacts with Pro-63, Arg-95, Glu-148, Val-161, Val-177, and Arg-197. It has been suggested that these contacts are required to stabilize the chromophore of eqFP611 in the *trans* configuration (16). In the ON state, a water molecule is located in the same place where the hydroxyl of the *p*-hydroxyphenyl group was found in the OFF state.

The side chains of Glu-148 and Thr-179 make a water-mediated hydrogen bond with the hydroxyl of the *p*-hydroxyphenyl moiety of the chromophore. This hydrogen bond, together with the stacking interaction between the hydroxyphenyl group and positively charged Arg-197, are possibly the important determinants stabilizing the *trans* configuration of chromophore and its anionic fluorescent state. Phenolic ring of the *trans* chromophores in mKate (19) and Rtms5 (21) makes stacking interaction with the guanidinium group of Arg-197. Similar stacking with positively charged His-197 is important for efficient fluorescence of amFP486 (22), KFP (23), and eqFP611 (16).

**Spectroscopic Properties of PAmCherry1.** In the OFF state, PAmCherry1 absorbs at 404 nm (Fig. S3) but does not fluoresce (13). After illumination with 405 nm violet light in ambient atmosphere, it became fluorescent, with the absorbance/emission peaks at 564 and 595 nm, respectively (13). In contrast, photoactivation of PAmCherry1 in the absence of oxygen was dramatically inhibited (Fig. S4). However, the photoactivation has been restored after returning the protein to the aerobic conditions.

The PAmCherry1 denaturation in the OFF state with 0.3 M HCl resulted in the absorbance spectra with 2 peaks at 341 and 397 nm. When denatured in 1 M NaOH, the dark PAmCherry1 had the absorbance spectra with 358 and 460 nm maxima (Fig. S3). In acid and alkaline conditions, the maxima were different from those observed for EGFP, mKate, TagRFP, and mCherry in the same denaturing conditions (Table S2). The spectroscopic data confirmed that PAmCherry1 in the OFF state contains a non-GFP-like and non-DsRed-like chromophore.

Denaturation of the photoactivated PAmCherry1 with 0.3 M HCl or 1 M NaOH resulted in the absorbance spectra with single peaks at 388 and 454 nm, respectively (Fig. S3). These absorbance characteristics were very similar to those observed for mKate, TagRFP, and mCherry in the acidic and alkaline conditions (Table S2), suggesting the chromophore of PAmCherry1 in the ON state has a chemical structure similar to that of the DsRed-like chromophore.

**Mutants of PAmCherry1 Affecting the Chromophore Formation.** To study properties of the chromophore, a mutagenesis of the amino acid residues of the chromophore-forming tripeptide and of its environment was carried out.

**Position 67.** To test whether the side chain of Tyr-67 is necessary to form the PAmCherry1 dark chromophore, we substituted Tyr-67 with several aliphatic residues including Leu and Gln. The substitution resulted in the mutants with the absorbance maxima at 407 nm, which were similar to that observed for PAmCherry1 in the OFF state (Table S3). Illumination of the mutants with 405 nm violet light did not result in their photoactivation or change of absorbance spectra. The data indicated that Tyr-67 does not form the $C^{\alpha}$-$C^{\beta}$ double bond. Interestingly, a spectrally similar chromophore, possibly also consisting of a single imidazolone ring with an N-acylimine bond, has been observed in a mutant of the cjBlue fluorescent protein with the Tyr67Leu substitution in the chromophore-forming tripeptide (24).

**Positions 70 and 197.** Crystallographic analysis of the photoactivated PAmCherry1 and mCherry indicate that positions 70 and 197 are close to the Tyr-67 $C^{\alpha}$-$C^{\beta}$ double bond and might participate in its formation. We performed mutagenesis of mCherry and introduced at these positions the amino acid residues found in PAmCherry1. An mCherry/K70N mutant was non-fluorescent. An mCherry/I197R mutant had red fluorescence but was less bright than mCherry. Both mutants were not photoactivatable by violet light.

Interestingly, the mCherry/K70N/I197R double mutant was dark but, after photoactivation, become fluorescent with the excitation/emission maxima at 575 and 601 nm, respectively (Table S3). It appears these 2 mutations are minimally required to convert mCherry into PAFP, suggesting that Lys-70 and Ile-197 play a role in the oxidation of the Tyr-67 $C^{\alpha}$-$C^{\beta}$ bond in mCherry.

**Positions 42 and 213.** To study an impact of the amino acid residues surrounding the putative N-acylimine on its formation, we further mutated the residues 42, 109, 111, and 213. PAmCherry1 mutants with Q213M,L,E,I substitutions were non-fluorescent and had the major absorbance maxima at 395 to 405 nm, which was similar to PAmCherry1 in the OFF state (Table S3). Illumination with 405 nm light converted them into red fluorescent state with absorbance at 552 to 560 nm. Similarly to dark PAmCherry1, the PAmCherry1/Q42L,V,T mutants did not fluoresce and absorbed at 398 to 413 nm. Their illumination with 405 nm light resulted in formation of red fluorescent chromophore with absorbance at 564 to 565 nm. These data suggested that positions 42 and 213 are not crucial for N-acylimine formation.

**Positions 109 and 111.** PAmCherry1/Q109A,V mutants did not absorb above 300 nm before and after illumination with violet light (Table S3). PAmCherry1/Q109L had traceable absorbance at 354 nm and, after illumination, exhibited a slight increase in the absorbance at 483 nm. The PAmCherry1/S111L,V,I variants absorbed at 383 to 384 nm. Their illumination with violet light resulted in a green chromophore with absorbance at 462 to 469 nm. Mutants PAmCherry1/Q109R/S111E and PAmCherry1/Q42L/Q109F/S111A had the absorbance maxima at 382 and 358 nm, respectively (Table S3). Their illumination with violet light resulted in a green fluorescence with the absorbance/emission maxima at 478 to 486 and 503 to 506 nm, respectively. In all mutants at positions 109 and 111, we did not observe any absorbance corresponding to the red chromophore, suggesting these positions are important for the N-acylimine formation.

**MS Analysis of PAmCherry1.** To further reveal chemical structures of the PAmCherry1 chromophore in the dark and photoactivated states we applied the denatured and chymo-trypsinized PAmCherry1 samples to MS. The mass spectra of the PAmCherry chromophore-bearing peptides in the OFF and ON states showed the mono-isotopic masses of 1244.4 and 1242.6 Da, respectively (Fig. S5). These masses corresponded to the predicted amino acid sequence of the chymotryptic peptide of PAmCherry1 $^{62}$SPQFMYGSNAY$^{72}$ with the chromophore-forming tripeptide Met-Tyr-Gly. The differences between the theoretical and observed masses of the peptides were 20 and 22 Da for the OFF and ON states, respectively. The reduction of 20 Da suggests the cyclization (i.e., loss of $H_2O$) and the single oxidation (i.e., $O_2$-mediated loss of $H_2$) of the $^{62}$SPQFMYGSNAY$^{72}$ peptide. The reduction of 22 Da suggests the cyclization (i.e., loss of $H_2O$) and the double oxidation (i.e., $O_2$-mediated loss of $2H_2$) of the peptide. Both PAmCherry1 peptides were isolated and subjected to further fragmentation by tandem MS by MALDI-TOF analysis to locate additional dehydrogenation site(s). The most prominent peaks in the secondary MS had masses indicated in Fig. S5. The fragment resulting from the cleavage at the $C^{\alpha}$-C bond in Met-66 of PAmCherry1 provided evidence whether and where the oxidation occurs (marked "i" in Fig. S5). This cleavage has been detected in MS/MS spectra of the DsRed and gtCP chromopeptides (17, 25).

The masses of the MS/MS fragments of the chromophore-bearing peptide of PAmCherry1 in the OFF state were consistent with the additional dehydrogenation between the $C^{a}$ and N atoms in Met-66. Hence, the chromophore of PAmCherry1 in the OFF state consists of the imidazolone cycle and the N-acylimine group and does not include side chain of Tyr-67 (Fig. S5*A*). The masses of the MS/MS fragments of the chromophore-bearing peptide of PAmCherry1 in the ON state located one dehydrogenation site between the $C^{a}$ and N atoms of Met-66 and another one between the $C^{\alpha}$ and $C^{\beta}$ atoms in Tyr-67. Thus, the chromophore of PAmCherry1 in the ON state consists of the (5E)-5-(4-hydroxybenzylidene)-3,5-dihydro-4H-imidazol-4-one and the N-acylimine group (Fig. S5*B*) that has been previously observed in DsRed (14, 15) and mCherry (14, 15), but in the *trans* configuration in PAmCherry1 (Fig. 1*B*).

The peptides $^{215}$ERAEGRHSTGGMDEL$^{229}$ and $^{215}$ERAEGRHSTGGMDELY$^{230}$ (the latter has Met-226 oxidized to methionine sulfoxide) from the C terminus of the dark PAmCherry1 had masses of 1,644.6 and 1,823.7 Da, respectively. After illumination of PAmCherry1 with 405 nm light, both peptides lost 44 Da, suggesting that one $CO_2$ molecule was released confirming the Glu-215 decarboxylation observed in the crystal structure. A quantitative Glu-215 decarboxylation was observed in the photoactivated PAGFP (12). The Glu-215 decarboxylation also occurred in the WT GFP (26) and in DsRed (27) but demanded the high-intensity illumination and was inefficient, indicating it was a side process. No decarboxylation of this residue has been detected in IrisFP PAFP even after the prolonged light irradiation (4). Thus, the data suggest that the Glu-215 decarboxylation is an important photochemical reaction accompanying the photoactivation of PAmCherry1.

## Discussion

The analysis of the PAmCherry1 chromophore and its environment allowed for the proposal of a mechanism for the formation of the PAmCherry1 chromophore and its photoactivation.

**Formation of the Dark Chromophore in PAmCherry1.** The first step is a cyclization of the chromophore tripeptide, resulting in formation of a colorless non-oxidized cyclized form. The next 2 steps result in the formation of the N-acylimine-containing the violet-absorbing OFF chromophore form (Fig. 3). The rate-determining reaction for formation of the OFF chromophore may be a deprotonation of the $C^{\alpha}$ of Met-66 in the cyclized form. In the dark PAmCherry1, Glu-215 activated by Arg-197 can serve as a general base for proton abstraction from $C^{\alpha}$ of Met-66. Because Glu-215 is positioned 4.5 Å away from $C^{\alpha}$ of Met-66, abstraction possibly occurs not directly but via water molecule and the main chain NH group of Ser-69, which is appropriately positioned over the $C^{\alpha}$ atom, resulting in the formation of reactive carbanion 1 (Fig. 3). The same water molecule can form hydrogen bonds with both the NH group of Ser-69 and carboxylate of Glu-215. Following proton abstraction from the $C^{\alpha}$ atom of Met-63, the proton transfers to Glu-215 through the NH group of Ser-69 and the water molecule. Formation of carbanion 1 is possible because the negative charge can be delocalized within the imidazol-5-ol and stabilized by a protonation of the $N^3$ atom of imidazol-5-ol by Glu-215 and by forming contacts with the positively charged side chain of Arg-95. Carbanion 1 corresponds to one of the common catalytic motifs, which involves carbanions stabilized by delocalization of negative charge into an adjacent imine that is polarized by the protonation (28). It has also been proposed that carbanion intermediate is involved in the formation of the DsRed chromophore (14).

Carbanion 1 then undergoes an oxidation by molecular oxygen. The oxidation reaction could proceed via a hydroperoxide intermediate, leading to the $H_2O_2$ release and proton abstraction from the NH group of Ser-69, possibly via water molecule coordinated by Gln-109 residue, substitution of which affected the N-acylimine formation. We hypothesize that the water molecule can further approach the NH group of Ser-69 because of their coordination with Gln-64 and Gly-68. The Ser-111 residue, which is important for the N-acylimine formation (as discussed earlier; see Table S3), may accept proton from Gln-109 and pass it via a chain of water molecules to the carbonyl group of the imidazolone or to Arg-95, which can be putative general bases for the proton abstraction (Fig. 3). The chain makes possible the equilibrium between 2 tautomeric

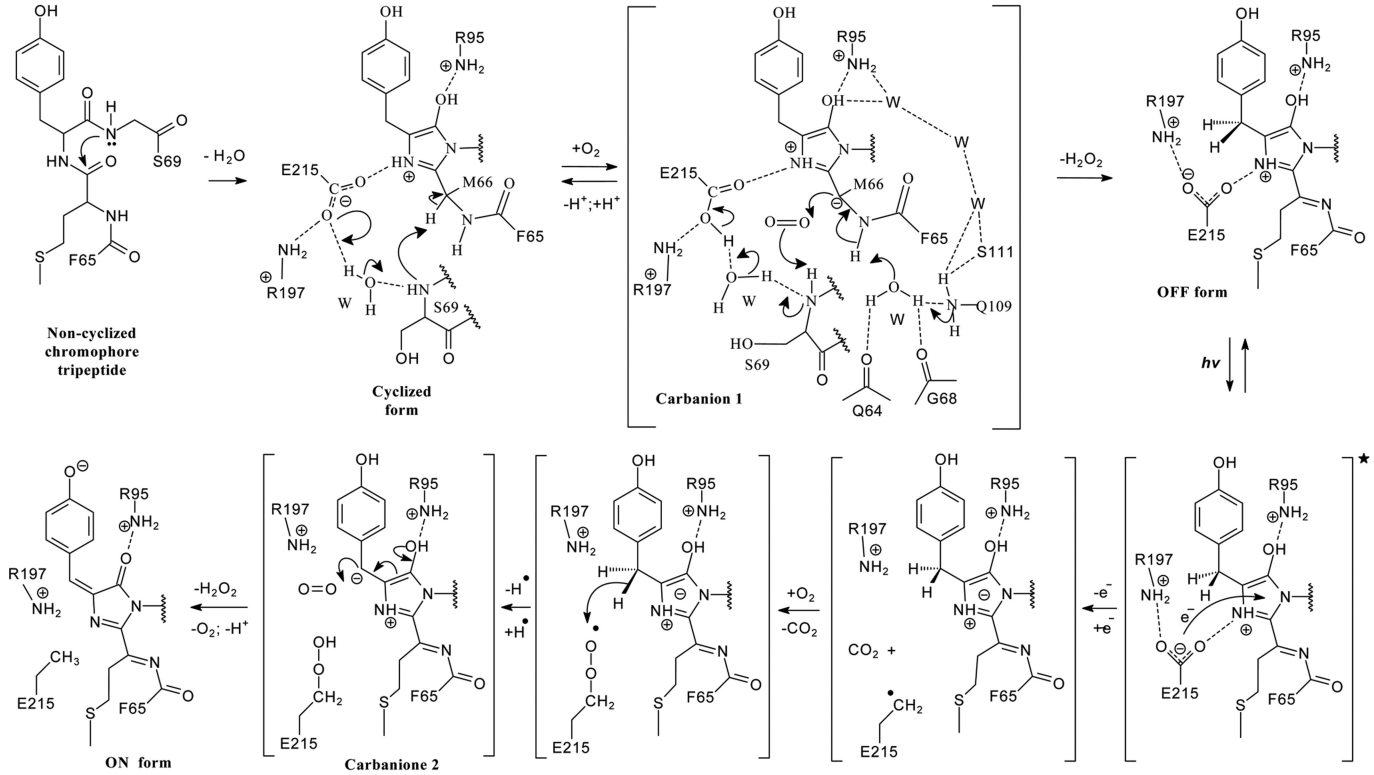


**Fig. 3.** Suggested mechanisms for the formation of the PAmCherry1 dark chromophore (OFF state) and its light-induced conversion into the fluorescent state (ON state) are shown. The cyclized form is the chromophore with the non-oxidized bond between *p*-hydroxyphenyl and imidazolone moieties and without N-acylimine. Hydrogen bonds are shown with dashed lines. Intermediate compounds are shown in parentheses. The chromophore in the excited state is denoted with asterisk. *hv*, indicates the illumination with violet light. Migration of the electron density is shown with curved arrows.

forms of the chromophore in the OFF state (Fig. S6). The imidazolone and Arg-95 are the only possible donor/acceptors of proton in the equilibrium. Finally, a stable product of the oxidation, the OFF form with N-acylimine, is formed.

A $H_2O_2$ molecule is typically produced in the course of carbanion oxidation processes. The $H_2O_2$ release during the formation of the GFP chromophore has been detected experimentally (29). The suggested here mechanism is also supported by the observation that a DsRed/Q66M mutant formed the N-acylimine more efficiently than DsRed (18). That was possible because hydrophobic Met-66 inhibited the formation of hydrogen bond between Glu-215 and Asn-42, resulting in the ability of Glu-215 to protonate the imidazol-5-ol ring (Fig. 3).

We cannot, however, exclude an alternative mechanism for the formation of the OFF state (Fig. S6), similar to that proposed for the GFP chromophore (29). In this alternative mechanism, an oxidation step precedes the tripeptide dehydration. The oxidation step suggests a proton abstraction from $C^{\alpha}$ of Tyr-67 with the formation of carbanion 1. Formation of carbanion 1 is possible because of the negative charge delocalization into the adjacent carbonyl group of 2-hydroxyimidazolidin-4-one, which forms a hydrogen bond with the positively charged side chain of Arg-95 (28). It has been suggested that Arg-95 is a general base for the proton abstraction in the GFP mechanism (29). In PAmCherry1, however, Arg-95 is located too far (4.7 Å) from the $C^{\alpha}$ atom of Tyr-67 (Fig. S7). It appears that Glu-215, which is activated by positively charged Arg-197 (as discussed earlier; see Table S3), is the only putative general base for proton abstraction from $C^{\alpha}$ of Tyr-67 located in its close proximity (3.9 Å). Then carbanion 1 undergoes an oxidation by molecular oxygen as described earlier. The next step in the alternative mechanism is the dehydration step, which could proceed via deprotonation of $C^{\alpha}$ of Met-66 in a hydroxylated cyclic imine (Fig. S6). Glu-215 activated by Arg-197 possibly abstracts proton from $C^{\alpha}$ of Met-66 via water molecule and the main chain NH group of Ser-69, which is appropriately positioned over the $C^{\alpha}$ atom. As the crystal structure of the OFF chromophore contains water molecule in the close proximity to both $C^2$ of the imidazolone (3.3 Å) and Glu-215 (2.8 Å), we propose that Glu-215 can protonate the leaving from the $C^2$ atom OH-group converting it into water.

**Mechanism of the PAmCherry1 Photoactivation.** The PAmCherry1 photoactivation results in an absorbance shift from 405 nm (OFF form) to 564 nm (ON form) (13), which could be explained by a conjugation of the electron systems of 2 aromatic rings via the $C^{\alpha}$-$C^{\beta}$ double bond in Tyr-67. A proton abstraction from the Tyr-67 $C^{\beta}$ atom is required to form this double bond. In the case of parental mCherry with the *cis* chromophore, Lys-70 is appropriately positioned over $C^{\beta}$ of Tyr-67 to serve as a general base for the proton abstraction from the $C^{\beta}$ atom. In PAmCherry1, Lys-70 is substituted with Asn-70. The K70N mutation in mCherry resulted in the non-fluorescent mutant, which was not photoactivatable. Consequently, the Asn-70 residue is likely not capable of proton abstraction, possibly, because it is a weaker proton acceptor comparing to Lys-70. In addition, Glu-148 in mCherry increases the Lys-70 acceptor properties via formation of hydrogen bond with this residue (15), whereas Asn-70 in PAmCherry1 has lost the contact with Glu-148 (Fig. S7). As the PAmCherry1 chromophore in the ON state adopts the *trans* configuration, it is possible that a proton or hydrogen abstraction occurs in a "*trans*-like" conformation of the OFF chromophore form. The most likely candidate for the abstraction in PAmCherry1 is the Glu-215 residue, because Glu-215 is the closest to the $C^{\alpha}$-$C^{\beta}$ single bond in Tyr-67 (Fig. S7). According

to the PAmCherry1 structure, the Glu-215 residue makes hydrogen bond with Arg-197, which, in turn, forms 2 hydrogen bonds with Glu-148. Consequently, Arg-197 in tandem with Glu-148 could activate Glu-215 for the proton or hydrogen abstraction. This mechanism is supported by the observation that the mCherry/K70N/I197R mutant, originally almost dark, exhibits red fluorescence after the photoactivation. The proton or hydrogen abstraction in PAmCherry1 and mCherry/K70N/I197R required violet light illumination, suggesting this abstraction was possible only with the chromophore in an excited state.

Because the PAmCherry1 photoactivation was accompanied by the Glu-215 decarboxylation, we propose a Kolbe-type radical mechanism for the transformation of the OFF form into the ON form. According to this mechanism, the OFF form of PAmCherry1 absorbs violet light and converts into an excited state. The PAmCherry1 chromophore in the excited state can act as an oxidant that accepts an electron from the anionic carboxylic group of Glu-215, resulting in the formation of a radical at the Glu-215 residue (Fig. 3). This radical is highly unstable, and Glu-215 rapidly decarboxylates with the formation of a [Glu-215-$CH_2$•] carbon radical. The latter radical is highly reactive and reacts with the first $O_2$ molecule with formation of a [Glu-215-$CH_2$-O-O•] radical. Consequently, the first $O_2$ molecule replaces the carboxylic group and makes a space for the second $O_2$ molecule. In other words, the decarboxylation of Glu-215 provides a vacancy for the second $O_2$ molecule to enter to the chromophore. The [Glu-215-$CH_2$-O-O•] radical possibly abstracts hydrogen from the Tyr-67 $C^{\beta}$ atom. In a PAmCherry1/A217S mutant, the hydroxyl group of Ser-217, which is located at 3.0 Å from the suggested [Glu-215-CH2•] radical, possibly competed with the first $O_2$ molecule for the reaction with [Glu-215-CH2•] that has resulted in approximately 30% of the PAmCherry1/A217S molecules after photoactivation remaining in the OFF state (Fig. S8). The hydrogen abstraction from the Tyr-67 $C^{\beta}$ atom forms carbanion 2, which is unstable and further oxidized by the second $O_2$ molecule to the ON form. In this radical mechanism, Arg-197 appears to cause deprotonation of the carboxylic group in Glu-215.

A quantitative decarboxylation of Glu-215 via the similar Kolbe-like mechanism was proven to occur during the PAGFP photoactivation (12). The PAGFP decarboxylation causes a dramatic rearrangement of the hydrogen bond network resulting in the chromophore deprotonation and, in turn, the photoactivation. In contrast, the photochemical decarboxylation of PAmCherry1 leads to the chemical oxidation with the double bond formation resulting in the red fluorescent chromophore.

## Conclusions

In this work, we demonstrate that PAmCherry1 does not belong to the existing 2 groups of irreversible PAFPs with the Kaede-like and PAGFP-like photoactivation mechanisms but defines a third group of PAFPs. We show that PAmCherry1 in the dark state has a non-fluorescent chromophore consisting of the imidazol-5-ol cycle conjugated with N-acylimine, but not with the phenolic ring of Tyr-67. The crystal structures and proposed photoactivation mechanism can be exploited to enhance photochemical characteristics of PAmCherry1 and to design PAFPs with emission in orange and far-red regions.

## Materials and Methods

The experimental procedures are briefly described here; a detailed description is provided in the *SI Materials and Methods*. PAmCherry1 and its mutants were expressed and purified as described (13). PAmCherry1 crystals (0.2 × 0.2 × 0.1 $mm^3$) were grown at 20 °C in 30% PEG 4000, 0.1 M Tris-HCl, 0.2 M $MgCl_2$ (pH 8.5). Photoactivation of crystals was performed with 405 nm laser at 50 $mW/cm^2$.

X-ray data were collected at 100 K at the X29A beam line (National Synchrotron Light Source, Brookhaven National Laboratory) or at the LRL-CAT (Advanced Photon Source, Argonne National Laboratory). Crystal structures were solved using the molecular replacement method with mCherry as a starting model.

PAmCherry mutants were produced using the QuikChange mutagenesis kit (Stratagene) in the pBAD/HisB vector (Invitrogen). Absorbance spectra were recorded on the U-3010 spectrophotometer (Hitachi).

For enzymatic digestion, a 20-$\mu$g aliquot of PAmCherry1 was added to 30 $\mu$L chymotrypsin in the buffer containing 0.1 M Tris-HCl, 10 mM $CaCl_2$ (pH 7.8), resulting in the enzyme:protein ratio of 1:60. The digest was incubated at room temperature for 22 h and quenched with 0.1% TFA. The peptides were desalted and isolated using the C18 ZipTip (Millipore).

Mass spectra were acquired on the 4800 MALDI TOF/TOF mass spectrometer (Applied Biosystems) equipped with the Nd:YAG laser (PowerChip JDS; Uniphase) operating at 200 Hz. MS/MS were acquired in the PSD mode with mass isolation window ±3 Da.

**ACKNOWLEDGMENTS.** We thank R. Y. Tsien for providing mCherry gene. This work was supported by National Institutes of Health Grant GM073913 (to V.V.V).

1. Betzig E, et al. (2006) Imaging intracellular fluorescent proteins at nanometer resolution. *Science* 313:1642–1645.
2. Chi KR (2009) Super-resolution microscopy: Breaking the limits. *Nat Methods* 6:15–18.
3. Nienhaus K, Nienhaus GU, Wiedenmann J, Nar H (2005) Structural basis for photo-induced protein cleavage and green-to-red conversion of fluorescent protein EosFP. *Proc Natl Acad Sci USA* 102:9156–9159.
4. Adam V, et al. (2008) Structural characterization of IrisFP, an optical highlighter undergoing multiple photo-induced transformations. *Proc Natl Acad Sci USA* 105:18343–18348.
5. Hayashi I, et al. (2007) Crystallographic evidence for water-assisted photo-induced peptide cleavage in the stony coral fluorescent protein Kaede. *J Mol Biol* 372:918–926.
6. Tsutsui H, et al. (2005) Semi-rational engineering of a coral fluorescent protein into an efficient highlighter. *EMBO Rep* 6:233–238.
7. Adam V, Nienhaus K, Bourgeois D, Nienhaus GU (2009) Structural basis of enhanced photoconversion yield in green fluorescent protein-like protein Dendra2. *Biochemistry* 48:4905–4915.
8. Gould TJ, et al. (2008) Nanoscale imaging of molecular positions and anisotropies. *Nat Methods* 5:1027–1030.
9. Patterson GH, Lippincott-Schwartz J (2002) A photoactivatable GFP for selective photolabeling of proteins and cells. *Science* 297:1873–1877.
10. Chudakov DM, et al. (2004) Photoswitchable cyan fluorescent protein for protein tracking. *Nat Biotechnol* 22:1435–1439.
11. Chudakov DM, Lukyanov S, Lukyanov KA (2007) Tracking intracellular protein movements using photoswitchable fluorescent proteins PS-CFP2 and Dendra2. *Nat Protoc* 2:2024–2032.
12. Henderson JN, et al. (2009) Structure and mechanism of the photoactivatable green fluorescent protein. *J Am Chem Soc* 131:4176–4177.
13. Subach FV, et al. (2009) Photoactivatable mCherry for high-resolution two-color fluorescence microscopy. *Nat Methods* 6:153–159.
14. Yarbrough D, et al. (2001) Refined crystal structure of DsRed, a red fluorescent protein from coral, at 2.0 Å resolution. *Proc Natl Acad Sci USA* 98:462–467.
15. Shu X, et al. (2006) Novel chromophores and buried charges control color in mFruits. *Biochemistry* 45:9639–9647.
16. Petersen J, et al. (2003) The 2.0 Å crystal structure of eqFP611, a far red fluorescent protein from the sea anemone Entacmaea quadricolor. *J Biol Chem* 278:44626–44631.
17. Gross LA, et al. (2000) The structure of the chromophore within DsRed, a red fluorescent protein from coral. *Proc Natl Acad Sci USA* 97:11990–11995.
18. Tubbs JL, Tainer JA, Getzoff ED (2005) Crystallographic structures of Discosoma red fluorescent protein with immature and mature chromophores: Linking peptide bond trans-cis isomerization and acylimine formation in chromophore maturation. *Biochemistry* 44:9833–9840.
19. Pletnev S, et al. (2008) A crystallographic study of bright far-red fluorescent protein mKate reveals pH-induced cis-trans isomerization of the chromophore. *J Biol Chem* 283:28980–28987.
20. Wilmann PG, et al. (2005) The 2.1 Å crystal structure of the far-red fluorescent protein HcRed: Inherent conformational flexibility of the chromophore. *J Mol Biol* 349:223–237.
21. Prescott M, et al. (2003) The 2.2 Å crystal structure of a pocilloporin pigment reveals a nonplanar chromophore conformation. *Structure* 11:275–284.
22. Henderson JN, Remington SJ (2005) Crystal structures and mutational analysis of amFP486, a cyan fluorescent protein from Anemonia majano. *Proc Natl Acad Sci USA* 102:12712–12717.
23. Quillin ML, et al. (2005) Kindling fluorescent protein from Anemonia sulcata: Dark-state structure at 1.38 A resolution. *Biochemistry* 44:5774–5787.
24. Chan MC, et al. (2006) Structural characterization of a blue chromoprotein and its yellow mutant from the sea anemone Cnidopus japonicus. *J Biol Chem* 281:37813–37819.
25. Martynov VI, et al. (2003) A purple-blue chromoprotein from Goniopora tenuidens belongs to the DsRed subfamily of GFP-like proteins. *J Biol Chem* 278:46288–46292.
26. Bell AF, Stoner-Ma D, Wachter RM, Tonge PJ (2003) Light-driven decarboxylation of wild-type green fluorescent protein. *J Am Chem Soc* 125:6919–6926.
27. Habuchi S, et al. (2005) Evidence for the isomerization and decarboxylation in the photoconversion of the red fluorescent protein DsRed. *J Am Chem Soc* 127:8977–8984.
28. Begley TP, Ealick SE (2004) Enzymatic reactions involving novel mechanisms of carbanion stabilization. *Curr Opin Chem Biol* 8:508–515.
29. Pouwels LJ, et al. (2008) Kinetic isotope effect studies on the de novo rate of chromophore formation in fast- and slow-maturing GFP variants. *Biochemistry* 47:10111–10122.